

# NJC

Accepted Manuscript



This is an *Accepted Manuscript*, which has been through the Royal Society of Chemistry peer review process and has been accepted for publication.

*Accepted Manuscripts* are published online shortly after acceptance, before technical editing, formatting and proof reading. Using this free service, authors can make their results available to the community, in citable form, before we publish the edited article. We will replace this *Accepted Manuscript* with the edited and formatted *Advance Article* as soon as it is available.

You can find more information about *Accepted Manuscripts* in the [Information for Authors](#).

Please note that technical editing may introduce minor changes to the text and/or graphics, which may alter content. The journal's standard [Terms & Conditions](#) and the [Ethical guidelines](#) still apply. In no event shall the Royal Society of Chemistry be held responsible for any errors or omissions in this *Accepted Manuscript* or any consequences arising from the use of any information it contains.



## A carboxylic acid functionalized benzimidazole-based supramolecular gel with multi-stimuli responsive properties

Hong Yao, Hong-Ping Wu, Jing Chang, Qi Lin, Tai-Bao Wei\* and You-Ming Zhang\*

Received 00th January 20xx,  
Accepted 00th January 20xx

DOI: 10.1039/x0xx00000x

www.rsc.org/

A novel supramolecular gelator (C11) based on a carboxylic-functionalized benzimidazole was synthesized, which could form an organogel (C11-OG) and generate a metallogel (Pb-MG) with Pb<sup>2+</sup>. Both of the two supramolecular gels have aggregation-induced enhanced emission (AIEE). The Pb-MG shows outstanding reversible sol-gel transitions induced by changing of temperature, EDTA and Na<sub>2</sub>S. It has the potential to be widely applied in materials science.

### 1. Introduction

Supramolecular gels are obtained by supramolecular self-assembly which is a spontaneous process that molecular aggregates into ordered nanostructures and provides a bottom-up approach to obtain structural regularity of various morphologies.<sup>1-9</sup> These self-assembly nanoscale structures of gelators, such as fibers, rods and ribbons, could entrap a large amount of organic solvent or water molecules to afford a solid-like appearance, namely, forming supramolecular organogels or hydrogels.<sup>10-16</sup> Among them, supramolecular organogels or hydrogels can be formed through non-covalent intermolecular interactions, such as hydrogen bonding,  $\pi$ - $\pi$  stacking, van der Waals, electrostatic interactions, and so on.<sup>17-20</sup> Benefited from the weak character of these forces, superamolecular gels have stimuli-responsive abilities<sup>21-24</sup> and can be used in chemosensors,<sup>25</sup> pollutant capture and removal, drug delivery and other applications.<sup>26-31</sup> Not only various supramolecular organogels and hydrogels have been reported so far, but those employing metal-ligand examples based on the concept of coordination chemistry have been also widely applied.<sup>32-34</sup>

It is widely accepted that heavy metal lead ion (Pb<sup>2+</sup>) is not only a serious problem for the environment but also for the health of human and other higher organisms due to its toxicity.<sup>35</sup> Pb<sup>2+</sup>, which is well known to act as a cumulative poison through water intake or food chains, can cause damage to the central nervous system, dysfunction in the kidneys and immune system of human beings, especially in children.<sup>36</sup> Therefore, the effective detection and removal of lead ion from the waste water has great practical interest.

In view of this, we reported a novel gelator (C11) which was

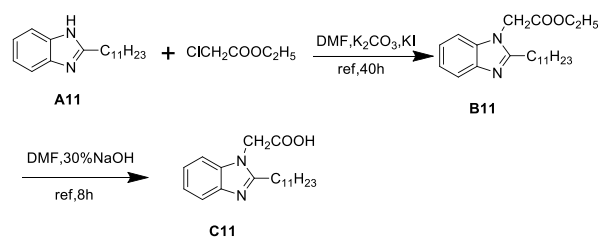
based on a benzimidazole unit as fluorescent signal group and carboxylic acid group as binding site.<sup>37</sup> Moreover, we rationally introduced the multi-self-assembly driving forces into the same gelator molecule, such as strong van der Waals existing in the long alkyl chains, hydrogen bonds existing in the carboxylic acid group and  $\pi$ - $\pi$  stacking existing in benzimidazole.

### 2. Synthesis and characterization of gelator C11

The synthesis of 2-hendecybenzimidazole(A11) was accomplished based on previous work<sup>38</sup> and the synthesis of C11 is shown in Scheme 1. 2-heptadecylbenzimidazole (1.36 g, 5 mmol) and K<sub>2</sub>CO<sub>3</sub> (0.6 g, 5 mmol), ethyl chloroacetate (0.61 g, 5 mmol) and KI (0.17 g, 1 mmol) were dissolved in appropriate absolute DMF and stirred 30 mins, respectively. Then they were blended and stirred at 90 °C for 40 h. After that, 20 mL NaOH water solution (w=30 %) was added as acid-binding agent. The mixture was stirred at 110 °C for 8 h. After cooling to room temperature, the solution was dispersed in 200 mL distilled water, and regulated pH to 1 to precipitate product. Afterwards, the solution was filtered and stoving to obtain a dry white powdery product C11. Finally, the residue was recrystallized from EtOH/H<sub>2</sub>O to give the product C11 (0.76 g, 46 %). m.p.: 149 °C. IR (KBr, cm<sup>-1</sup>):  $\nu$  3412, 2914, 2848, 1686, 1626, 1464, 1038, 744; <sup>1</sup>H NMR (DMSO-d<sub>6</sub>, 400 MHz)  $\delta$  1.59~1.62(t, 3H), 2.00~2.13 (m, 16H), 3.25~3.26 (m, 2H), 3.50~3.54 (m, 2H), 5.82 (s, 2H), 7.90~8.31 (m, 4H). <sup>13</sup>C NMR (DMSO-d<sub>6</sub>, 400 MHz):  $\delta$  20.39, 28.53, 32.66, 33.06, 35.13, 35.17, 35.25, 35.41, 35.45, 35.49, 37.73, 50.76, 116.20, 124.58, 127.73, 128.00, 141.93, 148.34, 161.81, 176.18. ESI-MS: calculated for (C11+H)+331.2 and found 331.3.

Key Laboratory of Eco-Environment-Related Polymer Materials, Ministry of Education of China; Key Laboratory of Polymer Materials of Gansu Province; College of Chemistry and Chemical Engineering, Northwest Normal University, Lanzhou, Gansu, 730070, P. R. China. E-mail: zhangnwnu@126.com, weitaibao@126.com; Tel.: +86-931-7973120.

Electronic Supplementary Information (ESI) available: [details of any supplementary information available should be included here]. See DOI: 10.1039/x0xx00000x



Scheme 1 Synthesis of gelator C11.

### 3. Results and discussion

#### 3.1 The formation process of supramolecular gel

The gelation abilities of gelator C11 were examined in various solvents by means of the “stable to inversion of a test tube” method. Interestingly, a steady blue-light-emitting supramolecular gel (C11-OG) is produced. C11 is found to form C11-OG in the presence of some protic mixing solvents, such as MeOH-H<sub>2</sub>O, EtOH-H<sub>2</sub>O and *i*-PrOH-H<sub>2</sub>O, and also form gels in the presence of polar aprotic solvents, such as acetone-H<sub>2</sub>O and DMF-H<sub>2</sub>O (Table 1). It may suggest that the hydrogen bonding between gelator and solvent molecules is crucial for the self-assembly process required for gelation.<sup>39</sup> Meanwhile, the van der Waals interactions between the alkyl chains of gelator and solvent molecules are equally significant.<sup>40-42</sup> The corresponding minimum gelator concentrations (MGCs) at room temperature were also measured. C11 exhibits excellent gelation abilities and low MGCs in MeOH-H<sub>2</sub>O or EtOH-H<sub>2</sub>O (*v/v*=1:1), and the MGCs is 0.9 % (w/v, 10 mg/mL=1%). The gel-sol transition temperature ( $T_{gel}$ ) was measured by using the ‘tilted tube’ method. The highest  $T_{gel}$  reaches a limit of 40 °C in EtOH-H<sub>2</sub>O. This process is thermoreversible and the gels are found to be stable in closed tubes for at least 3 months in room temperature.

Moreover, on addition of lead nitrate as Pb<sup>2+</sup> source to the C11 organogel (C11-OG) or mixing powder C11 and Pb(NO<sub>3</sub>)<sub>2</sub> in EtOH-H<sub>2</sub>O (*v/v*= 1 : 1), a stable Pb<sup>2+</sup>-coordinated metallogel (Pb-MG) was formed, accompanied with strong brilliant blue aggregation-induced fluorescence emission. The gelation properties of Pb-MG were also examined in different solvents (Table S1). This process is reversible because heating of the gel can lead to the formation of a liquid-like material. Interestingly, Pb-MG exhibits more excellent gelation abilities such as very low MGC in EtOH-H<sub>2</sub>O (*v/v*=1:1), and the MGCs of Pb-MG and C11-OG are 0.3 % and 0.9 % respectively. The gelation temperature ( $T_{gel}$ ) of the Pb-MG reaches 51 °C when the MGC of Pb-MG is just 0.3 wt %, while the  $T_{gel}$  of C11-OG is 40 °C when the MGC of C11-OG is 0.9 wt % (Fig.1). According to the MGCs and MGTs of C11-OG and Pb-MG, we can draw a conclusion that Pb-MG is more stable than C11-OG because of the coordination effect between C11 and Pb<sup>2+</sup>. Due to the existence of the coordination, the gel performance expresses more stable.<sup>43-44</sup>

Solvent	Gelation behavior <sup>a</sup>	Gelating time	MGC <sup>b</sup>	MGT <sup>c</sup>
MeOH	S	—	—	—
MeOH-H <sub>2</sub> O( <i>v/v</i> =1:1)	G	16 min	0.9	48
EtOH	S	—	—	—
EtOH-H <sub>2</sub> O( <i>v/v</i> =1:1)	G	15 min	0.9	40
<i>n</i> -PrOH	S	—	—	—
<i>n</i> -PrOH-H <sub>2</sub> O( <i>v/v</i> =1:1)	S	—	—	—
<i>i</i> -PrOH	S	—	—	—
<i>i</i> -PrOH-H <sub>2</sub> O( <i>v/v</i> =2:1)	G	10 min	1.0	40
<i>n</i> -BuOH	S	—	—	—
<i>t</i> -BuOH	SP	—	—	—
<i>i</i> -PeOH	S	—	—	—
Cyclohexanol	S	—	—	—
Acetone	S	—	—	—
Acetone-H <sub>2</sub> O( <i>v/v</i> =1:1)	G	9 min	0.9	46
Acetonitrile	SP	—	—	—
DMSO	S	—	—	—
DMSO-H <sub>2</sub> O( <i>v/v</i> =1:1)	SP	—	—	—
DMF	S	—	—	—
DMF-H <sub>2</sub> O( <i>v/v</i> =1:1)	G	7 min	1.0	48
Dichloromethane	SP	—	—	—
Chloroform	S	—	—	—
Carbon tetrachloride	SP	—	—	—

<sup>a</sup> G, gel ; S, solution ; SP, solution precipitate.

<sup>b</sup> MGC is the minimum gelator concentration. ( w/v%, 10 mg mL<sup>-1</sup> = 1 % )

<sup>c</sup> MGT is the gelation temperature(°C) at the minimum gelator concentration.

Table 1. Gelation properties of gelator C11

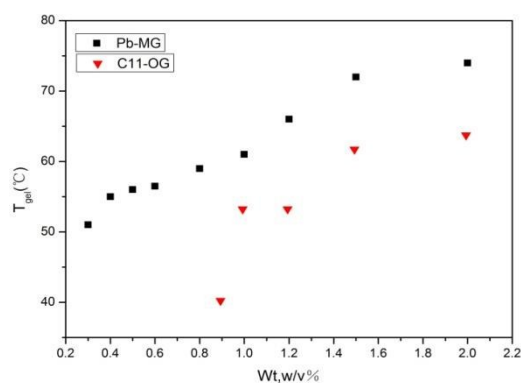
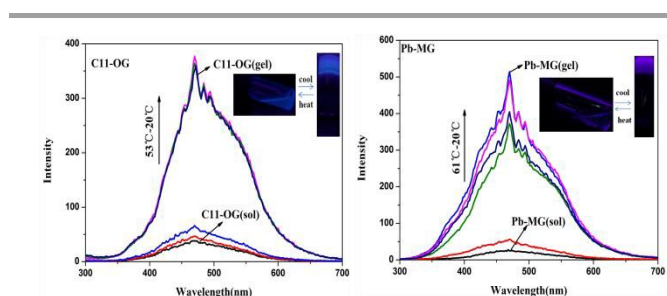


Fig. 1 Plots of  $T_{gel}$  at the different concentrations of organogel C11-OG and metallogel Pb-MG in EtOH-H<sub>2</sub>O (*v/v*= 1 : 1) (for Pb-MG, C11: Pb<sup>2+</sup> = 1 : 1)

### 3. 2 Aggregation-induced emission enhancement (AIEE)

As shown in Fig.2, C11-OG and Pb-MG (the concentration of gelator C11-OG and Pb-MG is 1 wt % respectively) have weak fluorescence in hot EtOH-H<sub>2</sub>O(v/v= 1 : 1) solution ( $T > T_{gel}$ ). However, with the temperature of the hot solution decreasing ( $T < T_{gel}$ ), the emission intensity at 470 nm shows an increase, which indicated that C11-OG and Pb-MG have aggregation-induced enhanced emission (AIEE) properties.<sup>45-47</sup> The photographs of sol-gel transformation illustrate that the solutions of C11-OG and Pb-MG emit very weak fluorescence, whereas gels emit strong brilliant blue aggregation-induced emission fluorescence. The fluorescence intensity of gels at 470 nm is about 5 times higher than that of solutions.



**Fig. 2** The temperature-dependent Fluorescence spectra of C11-OG (left) and Pb-MG (right, the molar ratio of C11/Pb<sup>2+</sup> = 1 : 1) in EtOH-H<sub>2</sub>O (v/v= 1 : 1) excited at 277 nm. The concentration of C11-OG and Pb-MG in the samples is 1 wt % respectively. Inset: photograph of the sol-gel transformation under 365 nm with a hand-held UV lamp.

### 3. 3 Self-assembly mechanism

Morphological features of the C11 powder, C11-OG and Pb-MG have been studied by using a field emission scanning electron microscopy (FESEM). Fig. 3(a) displays a morphology formed of rodlike aggregates of the powder C11. Fig. 3(b) shows overlapping rugate layer structure. The thickness of each layer was approximately 1  $\mu$ m of the C11-OG. In comparison with (a) and (b), we concluded that the morphology of the C11-OG can be changed by the presence of the gelation due to the self-assembly. Fig.3(c) shows the FESEM image of the Pb-MG in the presence of Pb(NO<sub>3</sub>)<sub>2</sub>. It can be clearly seen that the SEM image of (c) indicates the fibrous nature and intertwining of the fibers in 3-dimensions.

X-ray diffraction has also been carried out to understand the basic structure of the gel state (Fig.4(A)). Fig 4(A) shows the X-ray diffraction pattern of powder C11 and the dried gel obtained from Ethanol/water (1/1, v/v). The peak at  $2\theta = 25.04^\circ$  with the d value is 3.55Å of C11-OG suggests the presence of  $\pi$ - $\pi$  stacking interactions in the gel state.<sup>48</sup> Compared with the C11, for Pb-MG, a sharp diffraction peak was obtained in the big angle region at  $2\theta = 38.16^\circ$  which corresponds to a d-spacing of 2.36Å showing the bond length of Pb(II) and N-atom of benzimidazole groups, and  $2\theta = 32.40^\circ$  which corresponds to a d-spacing of 2.76Å indicating the bond length of Pb(II) and carbonyl oxygen atom of unprotonated carboxyl functional groups.<sup>49-50</sup> We also obtained a d-spacing of 3.65Å

by  $2\theta = 24.26^\circ$  of Pb-MG, it suggested the existence of  $\pi$ - $\pi$  stacking between aromatic nucleus. What's more, the d value of 17.9Å is less than twice as long as the theoretical alkyl chain length of C11 molecule,<sup>51-52</sup> belonging to the combination of two C11 molecules through hydrophobic interaction in each unit of the arrays.

The supramolecular interaction in the gel state can be ascertained by comparison of the FT-IR spectra of C11 powder and the Pb-MG xerogel (Fig4(B)). The strong absorption peaks at 1686 cm<sup>-1</sup> can be assigned to combined C=O stretching vibrations, indicating the presence of protonated carboxylic acids. The absorption peak at 1626 cm<sup>-1</sup> is the characteristic of C=N of benzimidazole. The peaks at 1686 cm<sup>-1</sup> corresponding to the carbonyl groups of free C11 showed obvious red shift after gelation. These changes suggest that metal ions had coordination with the carbonyl oxygen atom of protonated carboxyl functional groups and C=N groups of C11, respectively. The O-H stretching frequency of carboxylic acid of C11 powder (3412 cm<sup>-1</sup>) shifts to a lower frequency (3442 cm<sup>-1</sup>) for the Pb-MG xerogel, indicating strong intermolecular hydrogen bond.

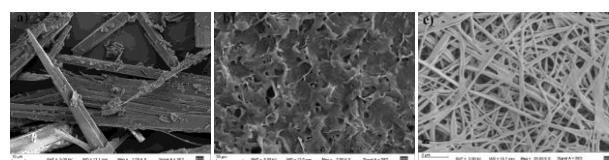


**Fig. 3** Comparative FESEM micrographs of (a) the powder of C11, (b) xerogel of C11-OG (obtained from 1 % organogel in EtOH-H<sub>2</sub>O(v/v= 1 : 1)), (c) xerogel of Pb-MG (obtained from 1 % EtOH-H<sub>2</sub>O(v/v= 1 : 1; C11/Pb<sup>2+</sup> = 1 : 1).

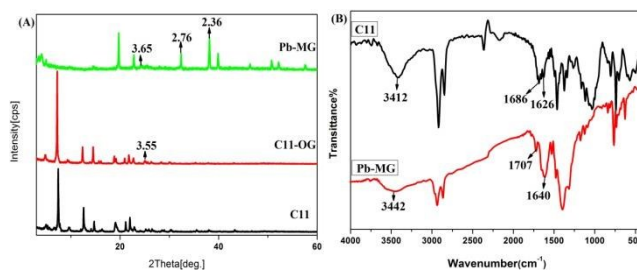


**Fig. 4** (A) Powder X-ray diffraction patterns for powder C11, xerogel of C11-OG (1 % in EtOH-H<sub>2</sub>O) and xerogel of Pb-MG (1 % in EtOH-H<sub>2</sub>O). (B) FTIR spectra of powder C11 and the xerogels of Pb-MG.

### 3. 4 Sol-gel transformations of Pb-MG by chemical stimuli

As expected, the Pb-MG is sensitive to temperature. Heating and cooling can result in a reversible gel-sol transition (Fig.5(A)). The reversible gel-sol transition could also be induced by adding appropriate chemicals. When the same equivalent EDTA was added to the Pb-MG, the Pb<sup>2+</sup> in Pb-MG might form a stable 1:1 complex with EDTA, which caused the complex between the C11 and Pb<sup>2+</sup> to disassemble accompanied its fluorescence intensity quenched when the gel turned into solution (Fig. S5). Later, when appropriate Pb(NO<sub>3</sub>)<sub>2</sub> was added, the supramolecular metallogel Pb-MG was recovered afterwards its fluorescence intensity enhanced at 468 nm. Furthermore, the addition of Na<sub>2</sub>S can also induce gel-sol transition because of the formation of black PbS precipitate.



The solution gradually returned to the gel state after adding appropriate equivalent  $\text{Pb}(\text{NO}_3)_2$  (Fig. S6). Finally, the fluorescence intensity could restore to the original state as shown in Fig 5(B). Undoubtedly,  $\text{Pb}^{2+}$  incorporated into the fibrillar networks, which have imparted the supramolecular Pb-MG multi-stimuli gel-sol transition sensitivity. Besides, the  $\text{Pb}^{2+}$  precipitate could be filtered. Therefore the gel can be used as a material to remove  $\text{Pb}^{2+}$ .

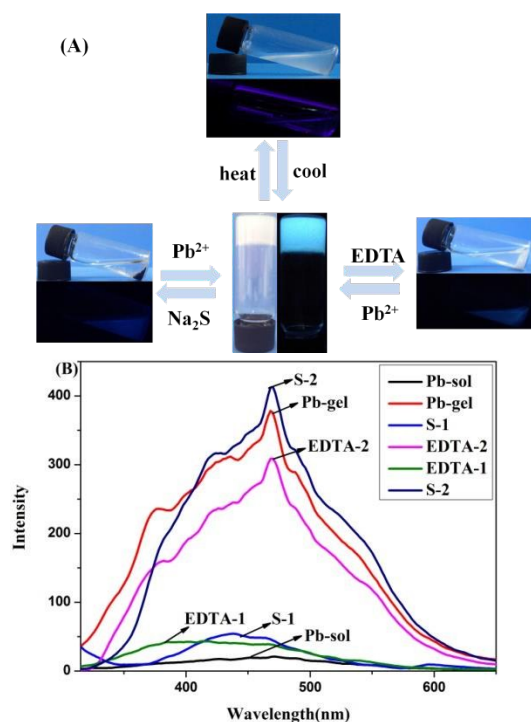
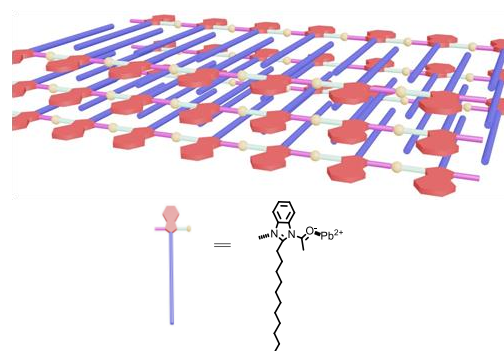


**Fig. 5.** (A) Illustration for reversible gel-sol transformation of Pb-MG by a variety of stimuli (temperature, chemical stimuli). (B) Fluorescence spectra of metallogels Pb-MG in sol and gel state (Pb-MG(sol) and Pb-MG(gel)): the sol and gel state of metallogels Pb-MG; S-1: the solution after addition of  $\text{Na}_2\text{S}$ ; S-2: the recovered gel after addition of  $\text{Pb}(\text{NO}_3)_2$  in the solution of S-1; EDTA-1: the solution after addition of EDTA; EDTA-2: the recovered gel after addition of  $\text{Pb}(\text{NO}_3)_2$  in the solution of EDTA-1).

In summary, on the base of the microscopic studies and the XRD results, it can be concluded that in the gelation process the C11-OG is possibly forming repeating bilayers in which are connected by the hydrophobic interaction in each unit of the arrays, intermolecular hydrogen bonding and  $\pi$ - $\pi$  stacking (Scheme S1). The possible interdigitated bilayer packing of the C11-OG is described in Scheme S1. For the Pb-MG the possible molecules are connected by metal-coordination and supramolecular self-assembly by intermolecular interactions, such as  $\pi$ - $\pi$  stacking and van der Waals (Scheme 2; Scheme S2). The results of ESI-MS (calculated for  $[\text{C11}+\text{Pb}(\text{NO}_3)_2\cdot 2\text{H}]$ : 659.7 and found 659.5) experiments also support this hypothesis (Fig. S4).



**Scheme 2** Schematic representation of the possible arrangement of metallogel Pb-MG.

## 4. Conclusion

In summary, we fabricated an organogel C11-OG and a novel metallogel Pb-MG. Both of them have strong blue AIEE in gel states. The Pb-MG showed efficient gelation ability toward EtOH- $\text{H}_2\text{O}$ , MeOH- $\text{H}_2\text{O}$  even at the gelator concentration as low as 0.3 wt %. We also found that the Pb-MG exhibits an interesting reversible gel-sol transition in response to temperature and chemical-stimuli. Based on SEM, IR and XRD studies, it has been demonstrated that coordination, hydrophobic interaction and  $\pi$ - $\pi$  stacking play a significant role in promoting the self-organization of C11-OG and Pb-MG in the gel state. Pb-MG showed good stimuli responsiveness toward the changes in  $\text{Na}_2\text{S}$  and EDTA. Moreover, because the gel was formed easily by gelator and a heavy metal ions Pb(II), it might provide the basis for heavy metal ion pollutant capture and removal, and also has the potential to be widely applied in other materials science.

## Acknowledgement

This work was supported by the National Natural Science Foundation of China (NSFC) (21064006; 21161018; 21262032), the Natural Science Foundation of Gansu Province (1010RJZA018) and the Program for Changjiang Scholars and Innovative Research Team in University of Ministry of Education of China (IRT1177).

## References

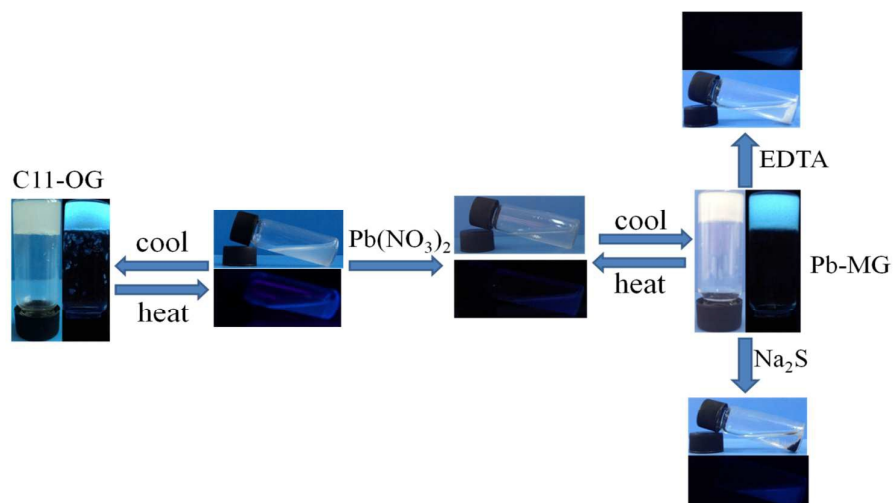
- 1 T.F. Jiao; Y.J. Wang; F.Q. Gao; T.X. Zhou; F.M. Gao, *Prog Nat Sci.* 2012, **22**, 64.
- 2 X. Ran; H.T. Wang; P. Zhang; B.L. Bai; C.X. Zhao; Z.X. Yu; M. Li, *Soft Matter.* 2011, **7**, 8561.
- 3 X.Z. Yan; D.H. Xu; X.D. Chi; J.Z. Chen; S.Y. Dong; X. Ding, Y.H. Yu; F.H. Huang, *Adv. Mater.* 2012, **24**, 362.
- 4 S.Y. Dong; Y. Luo; X.Z. Yan; B. Zheng; X. Ding; Y.H. Yu; Z. Ma; Q.L. Zhao; F.H. Huang, *Angew. Chem. Int. Ed.* 2011, **50**, 1905.
- 5 B.B. Shi; D.Y. Xia; Y. Yao, *Chem. Commun.* 2014, **50**, 13932.
- 6 X.Z. Yan; D.H. Xu; J.Z. Chen; M.M. Zhang; B.J. Hu; Y.H. Yu, F.H. Huang, *Polym. Chem.*, 2013, **4**, 3312.
- 7 B.B. Shi; K.C. Jie; Y.J. Zhou; D.Y. Xia; Y. Yao, *Chem. Commun.*, 2015, **51**, 4503.
- 8 S.Y. Dong; B. Zheng; D.H. Xu; X.Z. Yan; M.M. Zhang; F.H. Huang, *Adv. Mater.* 2012, **24**, 3191.

- 9 B.B. Shi; K.C. Jie; Y.J. Zhou; J. Zhou; D.Y. Xia; F.H. Huang, *J. Am. Chem. Soc.*, 2016, **138**, 80.
- 10 L. A. Estroff; A. D. Hamilton, *Chem. Rev.* 2004, **104**, 1201.
- 11 X.X. Ma; A.W. Yu; N. Tang; T.C. Wu, *Dalton Trans.* 2014, **43**, 9856.
- 12 P. Terech; R.G. Weiss, *Chem. Rev.* 1997, **97**, 3133.
- 13 R.G. Weiss, *J. Am. Chem. Soc.* 2014, **136**, 7519.
- 14 A.R. Hirst; B. Escuder; J.F. Miravet; D.K. Smith, *Angew. Chem. Int. Ed.* 2008, **47**, 8002.
- 15 S. Banerjee; R.K. Das; U. Maitra; *J. Mater. Chem.*, 2009, **19**, 6649.
- 16 J.W. Steed, *Chem. Commun.*, 2011, **47**, 1379.
- 17 Q. Lin; B. Sun; Q.P. Yang; Y.P. Fu; X. Zhu; Y.M. Zhang; T.B. Wei, *Chem. Commun.* 2014, **50**, 10669.
- 18 D. Yang; C.X. Liu; L. Zhang; M.H. Liu, *Chem. Commun.* 2014, **50**, 12688.
- 19 W.W. Fang; Z.M. Sun; T. Tu, *J. Phys. Chem. C.* 2013, **117**, 25185.
- 20 A.P. Sivadas; N.S. Saleesh Kumar; D.D. Prabhu; S. Varghese; S. Krishna Prasad; D.S. Shankar Rao; S. Das, *J. Am. Chem. Soc.* 2014, **136**, 5416.
- 21 W. Xia; M.F. Ni; C.H. Yao, X.L. Wang; D.Z. Chen; C. Lin; X.Y. Hu; L.Y. Wang, *Macromolecules.* 2015, **48**, 4403.
- 22 M.M. Zhang; D.H. Xu; X.Z. Yan; J.Z. Chen; S.Y. Dong; B. Zheng; F.H. Huang, *Angew. Chem. Int. Ed.* 2012, **51**, 7011.
- 23 A. Dey; S.K. Mondal; K. Birdha, *CrystEngComm*, 2013, **15**, 9769.
- 24 M.D. Segarra-Maset; V.J. Nebot; J.F. Miravet; B. Escuder, *Chem. Soc. Rev.*, 2013, **42**, 7086.
- 25 S. Barman; J.A. Garg; O. Blacque; K. Venkatesan; H. Berke, *Chem. Commun.*, 2012, **48**, 11127.
- 26 E. Busseron; Y. Ruff; E. Moulin; N. Giuseppone, *Nanoscale.* 2013, **5**, 7098.
- 27 H.H. Lee; S.H. Jung; S. Park; K.M. Park; J.H. Jung; *New J. Chem.* 2013, **37**, 2330.
- 28 Y. Furukawa; T. Ishiwata; K. Sugikawa; K. Kokado; K. Sada, *Angew. Chem. Int. Ed.* 2012, **51**, 10566.
- 29 M. Rodrigues; A.C. Calpena; D.B. Amabilino; M.L. Garduño-Ramírez; L. Pérez-García, *J. Mater. Chem. B.* 2014, **2**, 5419.
- 30 Y.M. Zhang; W.Q. Zhang; J.Q. Li; J.P. Dang; T.B. Wei, *Materials Letters*, 2012, **82**, 227.
- 31 S. Sengupta; R. Mondal, *J. Mater. Chem. A*, 2014, **2**, 16373.
- 32 B. Partha; C. Priyadarshi; S. Arnab; M. Sanjoy; R. Bappaditya; K. N. Arun, *Langmuir.* 2014, **30**, 7547.
- 33 Q. Lin; T.T. Lu; X. Zhu; B. Sun; Q.P. Yang; T.B. Wei; Y.M. Zhang, *Chem. Commun.* 2015, **51**, 1635.
- 34 S.J. James; A. Perrin; C.D. Jones; D.S. Yufit; J.W. Steed, *Chem. Commun.* 2014, **50**, 12851.
- 35 T.B. Wei; J.P. Dang; Q. Lin; H. Yao; Y. Liu; W.Q. Zhang; J.J. Ming; Y.M. Zhang, *Sci China Chem.* 2012, **55**, 2554.
- 36 A. Dairam; J. Limson; G. M. Watkins; E. Antunes; S. J. Daya, *Agric. Food Chem.* 2007, **55**, 1039.
- 37 H. Yao; X.M. You; Q. Lin; H.P. Wu; T.B. Wei; Y.M. Zhang, *Chinese J Chem.* 2014, **32**, 607.
- 38 W.O. Pool; H.J. Harwood; A.W. Ralston, *J. Am. Chem. Soc.* 1937, **59**, 178.
- 39 Y. Lan; M.G. Corradini; R.G. Weiss; S.R. Raghavan; M.A. Rogers, *Chem. Soc. Rev.* 2015, **44**, 6035.
- 40 T. Tu; W. Assenmacher; H. Peterlik; G. Schnakenburg; K. Heinz Dötz, *Angew. Chem., Int. Ed.* 2008, **47**, 7127.
- 41 C.C. Lu; S. K. Su, *Supramol. Chem.* 2009, **21**, 572.
- 42 Y.M. Zhang; X.M. You; H. Yao; Y. Guo; P. Zhang; B.B. Shi; X. J. Shi; Q. Lin; T.B. Wei, *Supramol. Chem.* 2014, **26**, 39.
- 43 Q. Lin; B. Sun; Q.P. Yang; Y.P. Fu; X. Zhu; T.B. Wei; Y.M. Zhang, *Chem. Eur. J.* 2014, **20**, 1.
- 44 Q. Lin; X. Zhu; Y.P. Fu; Y.M. Zhang; R. Fang; L.Z. Yang; T.B. Wei, *Soft Matter.* 2014, **10**, 5715.
- 45 V.K. Praveen; C. Ranjith; N. Armaroli, *Chem. Int. Ed.* 2014, **53**, 365.
- 46 X. Zhu; Q. Lin; J.C. Lou; T.T. Lu; Y.M. Zhang; T.B. Wei, *New J. Chem.*, 2015, **00**, 1.
- 47 A. Maity; F. Ali; H. Agarwalla; B. Anothumakkool; A. Das, *Chem. Commun.* 2015, **51**, 2130.
- 48 S. Brahmachari; S. Debnath; S. Dutta; P. Kumar Das, *Beilstein J. Org. Chem.* 2010, **6**, 859.
- 49 C. Gabriel; M. Perikli; C.P. Raptopoulou; A. Terzis; V. Psycharis; C. Mateescu; T. Jakusch; T. Kiss; M. Bertmer; A. Salifoglou, *Inorg. Chem.* 2012, **51**, 9282.
- 50 X.R. Meng; Y.L. Song; H.W. Hou; Y.T. Fan; G. Li; Y. Zhu, *Inorg. Chem.* 2003, **42**, 1307.
- 51 K.F. Wang; F.F. Jian; R.R. Zhuang; H.L. Xiao, *Cryst Growth Des.* 2009, **9**, 3934.
- 52 H. Yao; X.M. You; Q. Lin; J.J. Li; Y. Guo; T.B. Wei; Y.M. Zhang, *Chinese Chem Lett.* 2013, **24**, 703.

Graphical Abstract

## A carboxylic acid functionalized benzimidazole-based supramolecular gel with multi-stimuli responsive properties

Hong Yao, Hong-Ping Wu, Jing Chang, Qi Lin, Tai-Bao Wei\* and You-Ming Zhang\*



We fabricated an organogel C11-OG and a novel metallogel Pb-MG, both of the gels have strong blue AIEE in gel states.